Indian Journal of Geo Marine Sciences
Vol. 48 (07), July 2019, pp. 1098-1103

Underwater dual manipulators-Part I: Hydrodynamics analysis and computation

Mingjie Bi[1], Guoyuan Tang[1], Xianbo Xiang[1,2*], Guohua Xu[1], & Qin Zhang[3]

[1]School of Naval Architecture and Ocean Engineering, Huazhong University of Science and Technology, Wuhan, China
[2]Shenzhen Huazhong University of Science and Technology Research Institute, Shenzhen 518057, China
[3]State Key Lab of Digital Manufacturing, Equipment and Technology, Huazhong University of Science and Technology, Wuhan 430074, China
*[E-mail: xbxiang@hust.edu.cn]

This paper introduces two 4-DOF underwater manipulators mounted on autonomous underwater vehicle (AUV) with grasping claws, such that the AUV can accomplish the underwater task by using dual manipulators. Mechanical design of the manipulator is briefly presented and the feature of the simple structure of dual manipulators is simulated by using Solid Works. In addition, the hydrodynamics of the manipulator is analyzed, considering drag force, added mass and buoyancy. Then, hydrodynamic simulations of the manipulator are conducted by using 3-D model with Adams software, from which the torque of each joint is calculated. This paper presents an integrated result of computed torques by combining the theoretical calculation and simulation results, which is instrumental in determining the driving torque of the manipulators.

[Keywords: Underwater manipulator; Hydrodynamics; Simulation; Driving torque**]**

Introduction

With the development of marine technology and ocean exploration, underwater robotic vehicles and underwater manipulators play an important role in underwater operational tasks where human access is difficult[1,2,3,4,5]. Research work on modeling, control and simulations of intelligent control systems, including advanced ship[6], manipulator[7], aerial robot[8,9] and marine robot[10,11,12,13,14], attracts a lot of interest in robotic community. However, different from the manipulator on the ground, underwater manipulator suffers from the hydrodynamic effects in the water. Therefore, the dynamic model, especially hydrodynamics, is necessary to be analyzed.

In recent years, considerable research work on the underwater manipulator has been done. A 3-DOF underwater manipulator is introduced in Yu et al.[15]. Zhang et al.[16] introduced a hydrodynamic model to analyze the underwater manipulator, but the simulation doesn't cover the torque. Chang et al.[17] used Lie group to build a dynamic model of underwater vehicle-manipulator system (UVMS). Yuh et al.[18] identified four hydrodynamic forces which should be taken into consideration: Added mass, fluid acceleration, drag force, and buoyancy. Levesque et al.[19] calculated the drag forces and torques. Fossen et al.[20] introduced a simplified hydrodynamic model of underwater manipulator. Asghar et al.[21] analyzed the kinematic model of underwater manipulator. Gao et al.[22] illustrated the different influence of different hydrodynamic force and torque. Lin et al.[23] and Zou et al.[24] used Adams to simulate the kinematics model of two type of manipulator. However, due to the work limitations and purpose, these research works didn't utilize the hydrodynamic analysis to calculate the maximum torque of the joints.

In this paper, a 4-DOF underwater manipulator is introduced, including the overall structure. Then, on the assumption that manipulator velocity is slow and water is still, four hydrodynamic forces and torques are discussed. Simulations are performed to gain the torque curve and then the two results are combined to calculate the maximum driving torque.

Materials and Methods

UVMS design

In this paper, the UVMS consists of AUV and two underwater manipulators[25,26], which can grab or embrace the task target better than that using one. To reduce the flow resistance of the AUV, the two manipulators are mounted on both sides of the AUV, which are concave. In this way, the AUV also protects the two manipulators when they are not working. The two fixed points of the manipulators are interlaced, located at the front of the AUV, for the purpose that

the two manipulators can grasp the target more firmly. When seizing the target, the UVMS is able to carry it and move together.

Manipulator design

To balance the mass and structure, the 3-D model of the 4-DOF underwater manipulator is shown in Figure 2, consisting of shoulder, upper arm, lower arm, wrist and a claw as the end-effector. Considering the influence of water, the overall shape of the manipulator is designed as a cylinder and the material used is aluminum alloy.

The shoulder joint is perpendicular to the other joint, which is connected to the pedestal and used to make the manipulator out of the AUV. The other three joints are designed to ensure that the end-effector can reach different position in 3-D space. In addition, the motor in the wrist makes the claw open and close through the linkage mechanism.

Depending on the size of AUV and the function of the underwater manipulator, the length and rotating degree of joints are different. The length of the manipulator is 1.28 m and the mass is 12.5 kg. The main parameters of the parts are shown in Table 1.

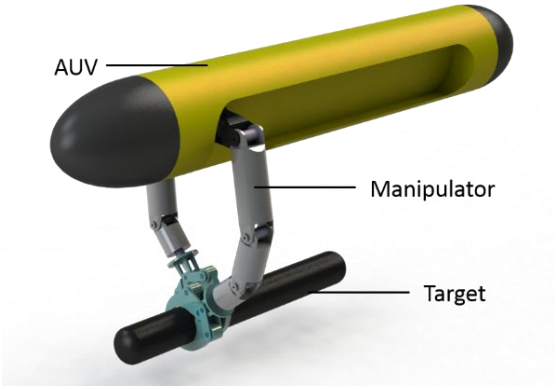

Fig. 1 — 3-D model of the UVMS

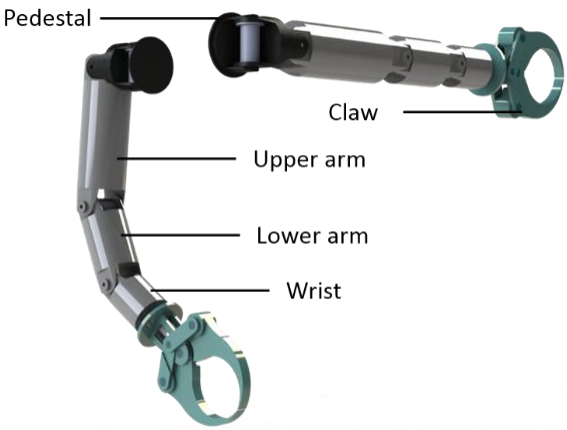

Fig. 2 — 3-D model of the underwater manipulator

Hydrodynamics analysis

The hydrodynamic analysis is based on several assumptions: The velocity of manipulator is slow; the water is still; and the manipulator is regarded as cylinder. Therefore, four torques should be taken into consideration, including drag torque, added-mass torque, gravity and buoyancy torque, and inertia torque[27].

Drag torque: According to fluid mechanics, when the object moves in the viscous liquid, the relative motion between them will cause liquid resistance. In this paper, the manipulator is regarded as cylinder, so the tangential drag force is small and negligible and only normal drag force is considered.

The coordinate system is shown in Figure 3, where l is the length and D is the diameter of the model.

The drag force and torque are calculated via the formula

$$df_D = \frac{1}{2}\rho C_D v^n(x)\|v^n(x)\|D\,dx \tag{1}$$

$$\tau_D = \frac{1}{2}\rho C_D \int_0^l([x\ 0\ 0]^T \times v^n(x))\|v^n(x)\|D\,dx \tag{2}$$

where C_D is the drag coefficient; $v^n(x)$ is the normal velocity vector of the cylindrical surface, which is the mapping of $v(x)$ on the *yoz* plane; D is the diameter of the thin rod; and dx is the thickness of the unit.

Added-mass Torque: When an object moves with acceleration in the water, the water will also be accelerated with the object. Therefore, the added-mass force is the reaction force of the object. The force and torque of added-mass are given as

$$df_A = \frac{\pi}{4}\rho C_m \frac{dv^n(x)}{dt} D^2\,dx \tag{3}$$

Table 1 — Parameters of the manipulator

Part	Length (m)	Diameter (m)	Thickness (m)	Rotation range(°)
Shoulder joint	0.08	0.12	/	0-90
Upper arm joint	0.37	0.11	0.01	0-90
Lower arm joint	0.22	0.10	0.01	0-40
Wrist joint	0.21	0.09	0.01	0-30

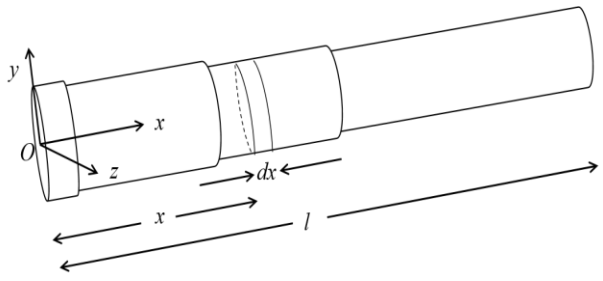

Fig. 3 — Model coordinate system

$$\tau_A = \frac{\pi}{4}\rho C_m \int_0^l ([x \quad 0 \quad 0]^T \times \frac{dv^n(x)}{dt}) D^2\, dx \tag{4}$$

where C_m is added-mass coefficient.

Inertia Torque: When the object is accelerated, there is inertia force at the mass center. As the manipulator is regarded as cylinder and the rotating axis is at the end of it, the moment of inertia is

$$I = \int r^2\, dm = \int_{x_1}^{x_2} \lambda x^2\, dx \tag{5}$$

where $\lambda = \frac{m}{l}$ is the mass line density.

Considering the cylinder is hollow, the mass of the model is

$$M = \rho' \pi (\left(\frac{D}{2}\right)^2 - \left(\frac{D}{2} - t\right)^2) l \tag{6}$$

where t and ρ' represent the thickness and density of the hollow cylinder.

Therefore, the inertia torque can be given as

$$T_I = I\alpha \tag{7}$$

where α is the angular acceleration.

Gravity and buoyancy torque: To simplify the calculation, buoyancy center coincides with the mass center. The gravity and buoyancy torque have the following form as

$$T_G = \sum M_i g d_i + \sum m_i g l_i \tag{8}$$

$$T_B = \sum \rho V_i g d_i + \sum \rho v_i g l_i \tag{9}$$

where M_i and V_i represent the mass and volume of the manipulator parts; m_i and v_i represent the mass and volume of the motor, and d_i and l_i represent the distance from mass center of manipulator parts and motor to the rotating axis.

Calculation result: Based on the parameter of the manipulator, the torque of all joints can be calculated. Through the analysis of the model, the driving torque of the joints is given as

$$T = \tau_D + \tau_A + T_I + T_G - T_B \tag{10}$$

Table 2—Calculated driving torque of joints

Shoulder joint	1.4075 N·m
Upper arm joint	51.6178 N·m
Lower arm joint	22.1166 N·m
Wrist joint	10.3730 N·m

Table 3—Parameters of simulation

Part	Angular velocity	Time	Acceleration /deceleration time
Shoulder joint	0.0977 rad/s	16 s	0.5 s
Upper arm joint	0.1042 rad/s	14 s	0.5 s
Lower arm joint	0.1506 rad/s	5.5 s	0.5 s
Wrist joint	0.2049 rad/s	1.5 s	0.5 s

In this paper, the rotating axis of shoulder joint is parallel to the gravity, so the driving torque doesn't include gravity and buoyancy torque. As for the other joints, the results are calculated using the formula.

The results are shown in Table 2.

Results and Discussion

Results

In this paper, the 3-D model is imported to the simulation software, which can compute the torque by simulating the motion. However, the 3-D modeling function of the simulation software is not strong as the modeling software, so the original assembly relationship of the models cannot be retained in the simulation software[28]. Therefore, the complicated structure of the claw has to be simplified, as shown in Figure 4.

In the simulation environment, the gravity and buoyancy exist and the added-mass force and drag force are placed on the point of them. Then, as the velocity of the claw is constant, the rotation processes of different joints are different. But all the joints rotate with the acceleration – uniform-deceleration process. The parameters of the simulation are shown in Table 3.

From the simulation process, as shown in Figure 5, we can know the position of manipulator when the torque is maximum.

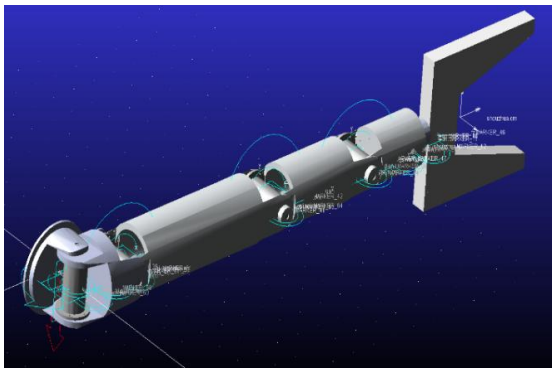

Fig. 4 — Model in simulation software

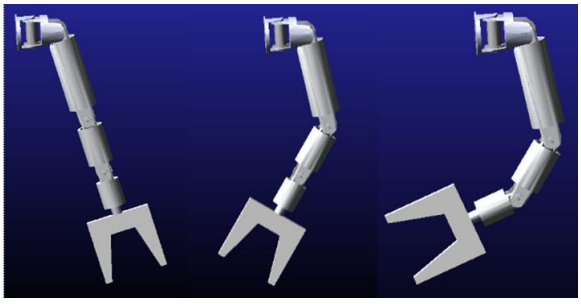

Fig. 5 — Simulation process

The simulation results are shown in Figure 6, which are the torque curves of different joints.

From the shape of the curves above, it is obvious that the gravity and buoyancy torques are much greater than other torques (except the shoulder joint). To figure out the influence of the other torques, the simulation need to be continued, not including gravity and buoyancy. The simulation results are shown in Figure 7

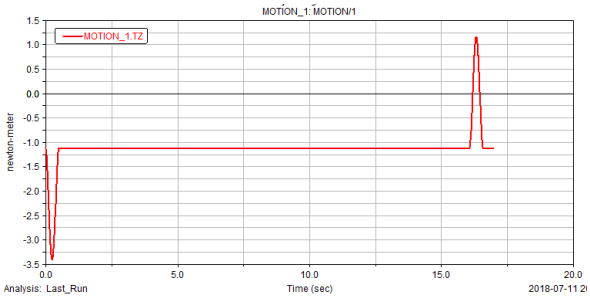

(a) Shoulder joint

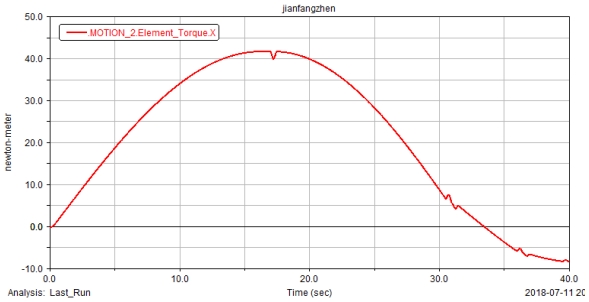

(b) Upper arm joint

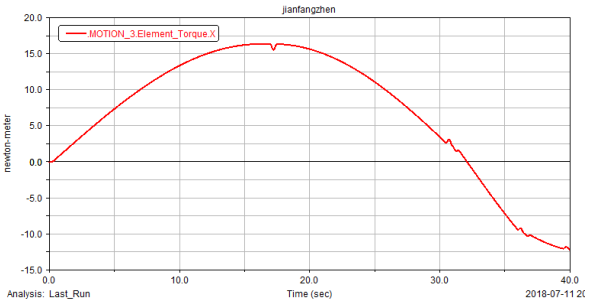

(c) Lower arm joint

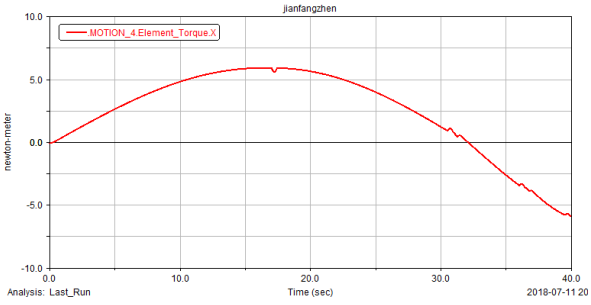

(d) Wrist joint

Fig.6 — Torque of different joints

Discussion

Due to the direction of the simulation process, the torque curves are similar to sine curve. But from Figure 6, we can know that the sudden change is the inertia torque, and the deviation to 0 is the sum of added-mass and drag torque.

Comparing the calculation results and simulation results, as shown in Table 4, we can analyze the difference between them and find some reasons:

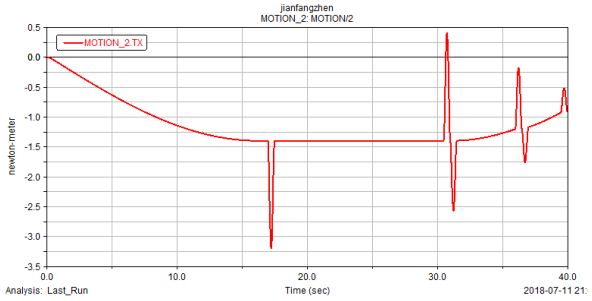

(a) Upper arm joint

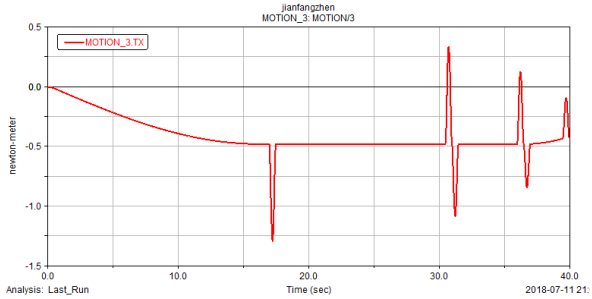

(b) Lower arm joint

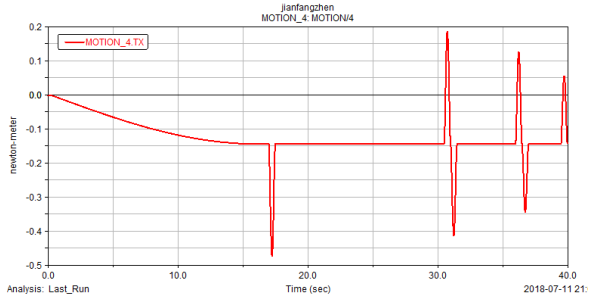

(c) Wrist joint

Fig.7 — Torque without gravity and buoyancy

Table 4 — Two results of driving torque

Part	Simulated result	Calculated result
Shoulder joint	3.4167 N·m	1.4075 N·m
Upper arm joint	41.7241 N·m	51.6178 N·m
Lower arm joint	16.3333 N·m	22.1166 N·m
Wrist joint	6.0021 N·m	10.3730 N·m

Table 5 — Driving torque of joints

Shoulder joint	3.3795 N·m
Upper arm joint	41.2779 N·m
Lower arm joint	16.2828 N·m
Wrist joint	5.9895 N·m

(1) In the simulation software, the mass of the model is calculate by the software, while in the theoretical calculation, the cylinder is not as accurate as the real manipulator.

(2) In the simulation software, the accelerating process is smoother. But when calculating the inertia torque, the acceleration is a constant.

(3) Limited by the function of the software, the added-mass force and drag force are placed on the model in an approximate way.

As mentioned in the preceding section, the two types of results both have deviation in some aspect. Therefore, we can select the accurate torque from the two results and calculate the driving torque more accurately. From the reasons (1) and (2), the gravity, buoyancy and inertia torques simulated by the software are more precise. While in the theoretical calculation, the added-mass and drag torques are better. By integrating the results, the relative accurate torques are shown in Table 5.

Conclusion

This paper presents a 4-DOF underwater manipulator, including structure and motion. Considering the influence of water, the hydrodynamic analysis is developed and the simulations of the manipulator are performed. The integral analysis provides a new way of calculating the driving torque of joints, which lays a foundation to the choice of motor.

Acknowledgment

This work was supported in part by the National Natural Science Foundation of China under Grant 51579111, in part by the Shenzhen Science and Technology Plan Project under Grant JCYJ201704I311305468, in part by the National Key Research and Development Program of China (Grant 2017YFB1302302) and in part by the Research Fund from Science and Technology on Underwater Vehicle Technology under Grant SXJQR2017KFJJ06.

References

1 Arshad, M.R., Recent advancement in sensor technology for underwater applications, *Indian J. Mar. Sci.*, 38(2009) 267-273.

2 Zhang, Q., Zhang, J.L, Chemori, A. &.Xiang, X.B., Virtual submerged floating operational system for robotic manipulation, *Complexity*, (2018) 1-18. DOI: 10.1155/2018/9528313

3 Lee, K.Q., Aminudin, A., Naomi, K., Pauziah, M., Tan, L.K. & Kang, H.S., Performance of two- and three-start helical strakes in suppressing the vortex-induced vibration of a low mass ratio flexible cylinder, *Ocean Eng.*, 166(2018) 253-261.

4 Kang, H.-S., Tang, C.H., Quen, L.K. & Yu, S.X, Parametric resonance avoidance of offshore crane cable in subsea lowering operation through A* heuristic planner, *Indian J. Geo Mar. Sci. 46 (2017) 2422-2433.*

5 Yahya, Mohd Faid; Arshad, Mohd Rizal, Switching target in position-based visual servoing for collision-free underwater docking of an autonomous underwater vehicle, *Indian J. Mar. Sci.*, 46(2017) 2452-2460.

6 Xiang, X.B., Yu, C.Y., Xu, H. and Zhu, Stuart X. Optimization of heterogeneous container loading problem with adaptive genetic algorithm. *Complexity*, 2018: 1–12. DOI: 10.1155/2018/2024184

7 He, W., Ouyang, Y.C. and Hong, J., Vibration control of a flexible robotic manipulator in the presence of input deadzone, *IEEE Transactions on Industrial Informatics*, 13(2017) 48-59.

8 Yu, C., Xiang, X.B., Wilson, P.A., & Zhang, Q., Guidance-error-based robust fuzzy adaptive control for bottom Following of a flight-style AUV with saturated actuator dynamics, *IEEE T Cybernetics*, (2019), DOI: 10.1109/TCYB.2018.2890582

9 Xiang, X.B., Liu, C., Su, H.S. & Zhang, Q., On decentralized adaptive full-order sliding mode control of multiple UAVs, *ISA Trans.*, 71(2017) 196-205.

10 Ye, Z., Hou, P. and Chen, Z., 2D maneuverable robotic fish propelled by multiple ionic polymer-metal composite artificial fins. *Int. Journal of Intelligent Robotics and Applications*, 2(2017) 195-208.

11 Chu, Z.Z., Xiang, X.B., Zhu, D.Q., Luo, C.M., Xie, D.. Adaptive Fuzzy Sliding Mode Diving Control for Autonomous Underwater Vehicle with Input Constraint. *International Journal of Fuzzy Systems*, 20(2018) 1460-1469

12 Phamduy, P., Vazquez, M., Kim, C., Mwaffo, V., Rizzo, A. & Porfiri, M., Design and characterization of a miniature free-swimming robotic fish based on multi-material 3D printing. *Int. Journal of Intelligent Robotics and Applications*, 2(2017) 209-223.

13 Yu, C.Y., Xiang, X.B., Lapierre, L. & Zhang. Q., Robust magnetic tracking of subsea cable by AUV in the presence of sensor noise and ocean currents, *IEEE J. Oceanic Eng.*, 43(2018) 311-322.

14 Yu, C.Y., Xiang, X.B., Zhang, Q. & Xu, G.H., Adaptive fuzzy trajectory tracking control of an under-actuated autonomous underwater vehicle subject to actuator saturation, *Int. J. Fuzzy Syst.*, 20(2018) 269-279.

15 Yu, Z.Y., Lei, J., Li, W.J., Xiang, Z.X., Wu, J.B., Design and Analysis of A Three-DOF Underwater Manipulator, paper presented at the *2011 International Conference on Fluid Power and Mechatronics*, (Beijing, China), pp.244-248, 2011.

16 Zhang, W.X., Design and Dynamic Analysis of an Underwater Manipulator, paper presented at the *China Academic Conference on Intelligent Automation*, (Fuzhou, China), pp.388-398, 2015.

17 Chang, Z.Y., Chen, B.C. & Yuan, P., Dynamic Modeling of Underwater Vehicle-manipulator System Based on Lie

Group, paper presented at the *Seventh International Conference on Design and Manufacturing Science*, (Guangzhou, China), pp.176-179, 2006.

18 Yuh, J., Modeling and control of underwater robotic vehicles. *IEEE Trans. Syst. Man Cybern.*, 20(1990) 1475-1483.

19 Lévesque, B., Richard, M.J., Dynamic analysis of a manipulator in a fluid environment. *Int. J. Robot Res*., 13(1994) 221-231.

20 Fossen, T.I., Guidance and control of ocean vehicles. (1994) Wiley, Hoboken.

21 Asghar, K. Forward Kinematic Modeling and Analysis of 6-DOF Underwater Manipulator, paper presented at the *2015 International Conference on Fluid Power and Mechatronics*, (Harbin, China), pp.1082-1085, 2015.

22 Gao, H., Zhang, M.L., Zhang, X.J., Li, Q., Research on Underwater Manipulator Dynamics Model and Torque Influence, *Machinery Design & Manufacture*, 3 (2017) 114-117.

23 Lin, H.B., Wang, Y.B., Zhang, Y., Dynamics analysis of the manipulator based on ADAMS, *Manufacturing Automation*, 11(2012) 80-83

24 Zou, P.H., Research on Underwater Manipulator ADAMS, *Robot Technology*, 4(2017) 52-53.

25 Christian, S., Yiannis, K., Lazaros, N., Xavi, G., Peng, Q., Dimos, V. D., Danica, K., Dual arm manipulation—A survey. *Robotics and Autonomous Systems*, 60(2012) 1340-1353.

26 Simetti, E. & Casalino, G., Whole body control of a dual arm underwater vehicle manipulator system. *Annual Reviews in Control*, 40(2015) 191-200.

27 Yue, P., Zhang, Q.F., An, X.W., Qu, F.J., Structure Design of 7F Underwater Electric Manipulator and Feasibility Analysis, *Machinery Design & Manufacture*, 4 (2014) 114-117.

28 Pan, D.Z., Wang, Q.M., Song, R.H., Yao, X., Gu, Y.H., Kinematics analysis and simulation on Underwater Manipulator, *Shipbuilding of China*.,1 (2009) 122-127.